Article ID: 1007－4627(2009)Suppl.－0094－06

MeV- and Sub-MeV-photon Sources Based on Compton Backscattering at SPring-8 and KPSI-JAEA*

K. Kawase[1], M. Kando[1], T. Hayakawa[1], I. Daito[1], S. Kondo[1], T. Homma[1], T. Kameshima[1], H. Kotaki[1], L. Chen[1], Y. Fukuda[1], A. Faenov[1], T. Shizuma[1], S. V. Bulanov[1], T. Kimura[1], T. Tajima[1], M. Shoji[2], S. Suzuki[2], K. Tamura[2], H. Ohkuma[2], Y. Arimoto[3], T. Yorita[4], M. Fujiwara[4], S. Okajima[4]

(1 *Kansai Photon Science Institute, Japan Atomic Energy Agency*, 8-1 *Umemidai, Kizugawa, Kyoto* 619-0215, *Japan*;
2 *Japan Synchrotron Radiation Research Institute*, 1-1-1 *Kouto, Sayo-cho, Sayo, Hyogo* 679-5198, *Japan*;
3 *Department of Physics, Osaka University*, 1-1 *Machikaneyama-cho, Toyonaka, Osaka* 560-0043, *Japan*;
4 *Research Center for Nuclear Physics, Osaka University*, 10-1 *Mihogaoka, Ibaraki, Osaka* 567-0047, *Japan*)

Abstract: Recently we have constructed two facilities for generating photon beams in the MeV and sub-MeV energy regions by means of the Compton backscattering with a laser and an electron beam at SPring-8 and at Kansai Photon Science Institute of Japan Atomic Energy Agency(KPSI-JAEA). The MeV-photon source at SPring-8 consists of a continuous-wave optically-pumped far infrared laser with a wavelength of 118.8 μm and an 8 GeV stored electron beam. Present MeV-photon flux is estimated to be 1.3×10^3 photons/s. On the other hand, the sub-MeV-photon source at KPSI-JAEA consists of a pulse Nd：YAG laser with a wavelength of 1 064 nm and a 150 MeV electron beam accelerated by microtron. In the first trial of the photon production in this source, backscattered photon flux is estimated to be 20 photons/pulse. Both the Compton backscattered photon sources have possibilities to be used for new tools in various fields such as nuclear physics, materials science, and astronomy.

Key words: laser Compton backscattering; polarized γ-ray; polarized X-ray

CLC number: O571.41$^+$8 **Document code**: A

1 Introduction

Compton backscattered photon sources recently have been developed at many facilities. The remarkable features of the photon beams from these sources are well-collimated and highly polarized. The schematic diagram of the Compton backscattering with a high energy electron beam and a laser is shown in Fig. 1. The Compton backscattered photon sources are used for various fields of research such as hadron physics at SPring-8[1], nuclear physics at Duke University[2], and biology at Lowrence Livermore National Laboratory[3].

In this paper, we report the present status of the MeV photon source developed at SPring-8, and the sub-MeV photon source at Kansai Photon Science Institute of Japan Atomic Energy Agency

* **Received date**: 13 Aug. 2008

* **Foundation item**: Japan Society for Promotion of Science under Grant-and Aid for Scientific Research(14205018); Ministry of Education, Science, Sports and Culture of Japan under Grant-and-Aid for Specially Promoted Research (15002013)

Biography: K. Kawase(1978－), male(Japanese Nationality), Osaka, Japan, Post-doctoral Fellow, working on the field of laser-plasma physics, beam physics, and nuclear physics; E-mail: kawase.keigo@jaea.go.jp

(KPSI-JAEA).

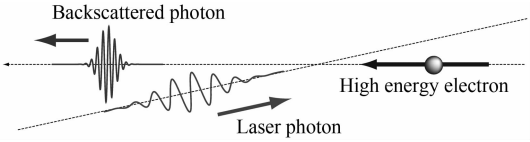

Fig. 1 The schematic diagram of the Compton backscattering.

2 MeV Photon Source at SPring-8

In order to generate MeV-photons based on the Compton backscattering with the 8 GeV electron beam at SPring-8, a far infrared(FIR) laser is needed. Thus, we adopt a continuous-wave(CW) optically-pumped methanol laser with a wavelength of 118.8 μm. This laser is pumped by a CO_2 laser with an output power of over 200 W. The CW-output power of the FIR laser is 1.6 W at maximum. The schematic diagram of the FIR laser system is shown in Fig. 2.

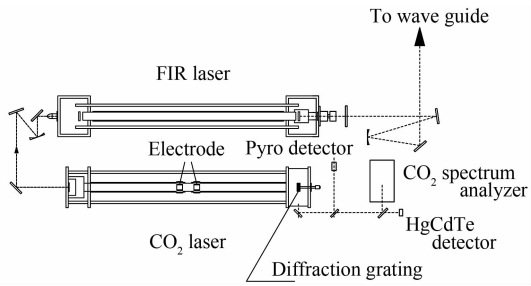

Fig. 2 The schematic diagram of the FIR laser system.

Laser light is transported to the front-end of beamline at the electron storage ring tunnel by using dielectric wave guides. At the front-end, the laser is injected to the vacuum area by using focusing optics, and the laser is focused at the interaction point with the electron beam. In order to avoid the absorption of the laser light by atmospheric vapor, the laser transport line is filled with dry air, and kept with a dew point of under 50 ℃. As a result of this very low humidity environment, the laser transmittance to the front end is obtained to be 0.77.

The generated γ-rays are measured at the optics hatch of the beamline. In order to reduce the background due to the scattering of synchrotron radiation from the various components at the beamline, a lead shield box is installed, and a detector is mounted inside this box. The opening angle of the γ-ray detection is defined by using the lead collimator with a thickness of 5 cm. The collimator hole is 10 mm. The schematic diagram of the γ-ray detection setup is shown in Fig. 3.

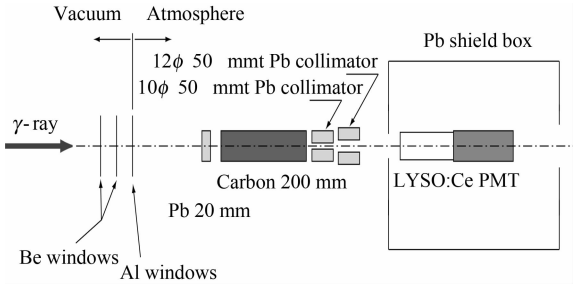

Fig. 3 The schematic diagram of the detector setup.

As the detector for the MeV γ-rays, we select the LYSO scintillator. This scintillator has fast time response with a decay time of 40 ns, and is made of high-Z materials.

After scanning the alignment of the laser path, we confirm the generation of the Compton backscattered γ-rays with a maximum energy of 10 MeV. In order to evaluate the γ-ray yield at the point where the electron beam collides the FIR laser, the Monte Carlo simulation of the detector response for the calculated Compton scattered γ-ray spectrum is made by using EGS4 simulation code[4, 5]. Comparing with the measured spectrum of the Compton scattered γ-rays and the result of the simulation, we find that the γ-ray yield at the collision point is 1.3×10^3 photon/s. The measurement and simulation results are shown in Fig. 4.

On the other hand, we also estimate the γ-ray flux at the collision point from the input laser power, laser profile, and the laser transmittance. That value is estimated to be 1.8×10^3 photon/s. The two values from the different view points are almost equal. Hence, this estimation of the γ-ray yield shows a reliable result.

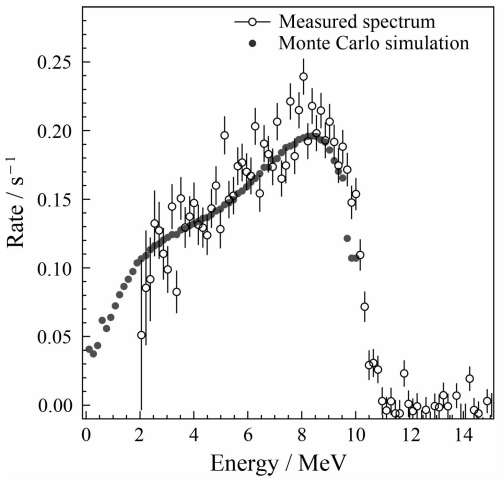

Fig. 4 MeV γ-ray spectrum obtained from the Compton backscattering between 8 GeV electron beam and 118.8 μm methanol laser. This spectrum is the net MeV γ-ray spectrum subtracted the background.

As the future prospects, the upgrading of the MeV γ-ray source at SPring-8 is on going. We will move the γ-ray generation system to a new beamline with a straight section at the storage ring. By using the straight section, we can use a long interaction region up to 16 m between the electron beam and the laser. We will also improve the laser transport with less laser loss to the interaction region. After the upgrade of the γ-ray source, we shall achieve the γ-ray flux to be at least 10^5 photons/s.

3 Sub-MeV Photon Source at KPSI-JAEA

At the present, there exist a few photon sources based on the Compton backscattering covering the energy region in sub-MeV. The polarized photon source in sub-MeV region is, however, required from various fields such as astrophysics, nuclear physics, and materials science. Thus, we try to make a photon source in the sub-MeV energy region via the Compton backscattering by using a 150 MeV microtron accelerator and a commercially available Nd : YAG laser with a wavelength of 1 064 nm. The maximum energy of the X-ray is estimated to be 400 keV.

The electron beam is accelerated by the microtron accelerator to 150 MeV with a pulse duration of 10 ps(rms), and is focused at the interaction point. The charge of the electron beam is 60 pC/pulse. The laser is also focused at the interaction point with an incident angle of 16°. The laser energy is 1 J, and the pulse duration of the laser is 23 ns(FWHM). After the collision, the generated X-rays go to the downstream of the electron beamline, and are detected by a scintillator or some X-ray detector. Both the electron beam and the laser are operated in 10 Hz, and they are synchronized with each other. The schematic diagram of the experimental setup is shown in Fig. 5.

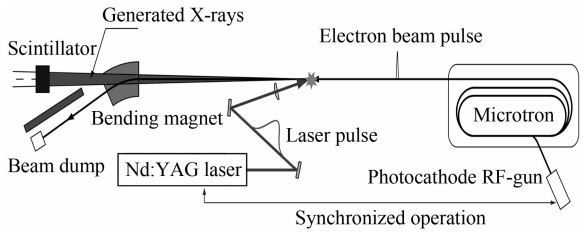

Fig. 5 The schematic diagram of the experimental setup for the generation of the Compton scattered X-rays with the energy of sub-MeV.

One of the most featuring points in this experiment is a precise collision alignment between the electron beam and the laser pulse by using a CCD spot monitor optics. For the electron beam, a high sensitive phosphor screen(LANEX, Kodak) is inserted at the focal point, and the image of the electron beam spot is observed by using the spot monitor optics. For the laser pulse, the spot is observed by using the same monitor optics attenuated after the focal point. The schematic diagram of the spot monitor optics is shown in Fig. 6. The typical spot diameters of the electron beam and the laser pulse are 400 and 100 μm , respectively. The results of the spot measurement for the electron beam and the laser pulse are shown in Fig. 7. This method provides precise collision point, and thus, we succeed in the generation of the Compton backscattered X-rays.

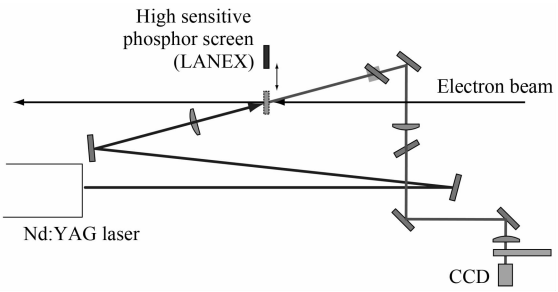

Fig. 6　The schematic diagram of the spot monitor optics.

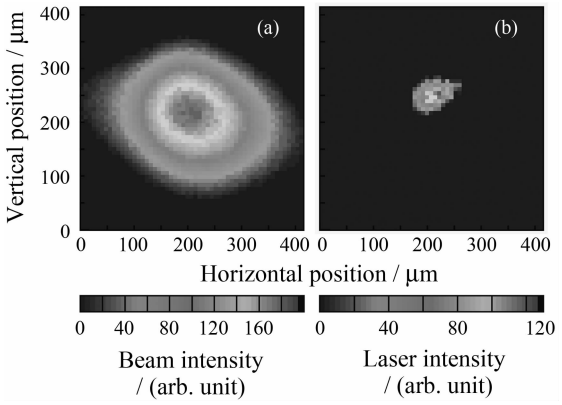

Fig. 7　Spot images of the electron beam and the laser pulse. (a) the electron beam spot image. The diameter of the electron beam spot is 400 μm. (b) the laser spot image. The diameter of the laser spot is 100 μm.

First of all, in order to confirm the X-ray generation, we use an imaging plate. The results of this measurement are shown in Fig. 8. As the result, we clearly confirm the generation of the backscattered X-rays. From the result of the imaging plate measurement, the angular divergence of the generated X-rays is estimated to be 3 mrad. This value is consistent with the theoretically estimated one from the Klein-Nishina formula. And the X-ray yield is also estimated from the imaging plate result to be (45±20) photons/pulse.

We also try to measure the generated X-rays by using a scintillator. At first, we try to use a typical inorganic scintillator, NaI, but we cannot measure the generated X-rays due to the huge background from the electron beam dump. Thus, we use an LYSO scintillator which has a relatively high light-output with a decay time of 40 ns, and is made of high-Z materials. By using the LYSO scintillator, we succeed in the separation of the signals and the delayed huge background.

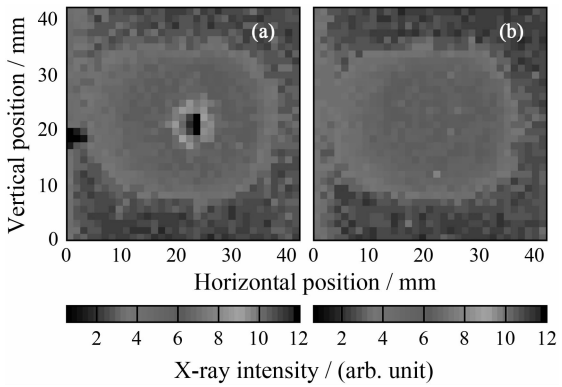

Fig. 8　The results of the measurement of the backscattered X-rays by using imaging plates. (a) laser on case. (b) laser off case. The irradiation time for each case is 2 h. In the laser on case, the generated X-ray image is clearly observed in the center of the imaging plate comparing the laser on case and the laser off case.

Although the delayed huge background is separated from the signals, the signals and other background are simultaneously enter the LYSO within the pico-second order. Thus it is difficult to make the spectral measurement for the generated X-rays. Therefore, we measure the total photon energy in one pulse by using the LYSO. In this measurement, the laser is operated in 5 Hz synchronized with the 10 Hz electron beam. This alternate laser operation reduces the systematic errors in the measurement data.

The difference of the mean values for the distributions of the total photon energy between in the laser injected case and laser non-injected case corresponds to the mean energy of the total backscattered photons in one-pulse. The result of the LYSO measurement is shown in Fig. 9. By using the calculated spectrum of Compton backscattered photons and the detector efficiency estimated with the EGS4 simulation code[4, 5], we obtain the total generated X-ray flux to be (20±10) photons/s. This flux is consistent with the previous flux estimated on the basis of the measurement by using imaging plates within the error bars. Therefore,

we believe that the estimation for the generated X-ray flux is reliable.

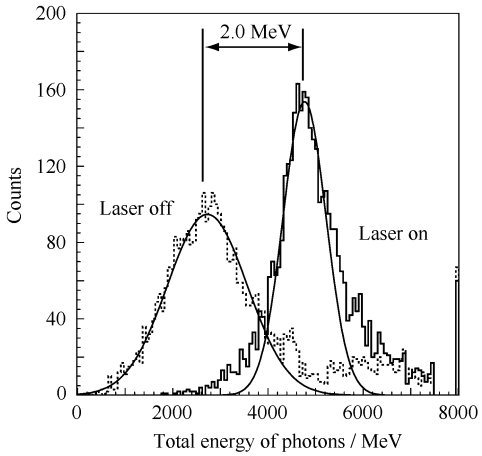

Fig. 9 The result of the measurement of the generated X-rays by using the LYSO scintillator.

One of the features of the Compton backscattered photons is that the generated photons have the definite polarization. The polarization of the backscattered photons is determined by the incident laser polarization. Thus, by changing the direction of the linear polarization of the incident laser by using a half-wavelength wave plate, the direction of the linear polarization of the backscattered photons is easily changed.

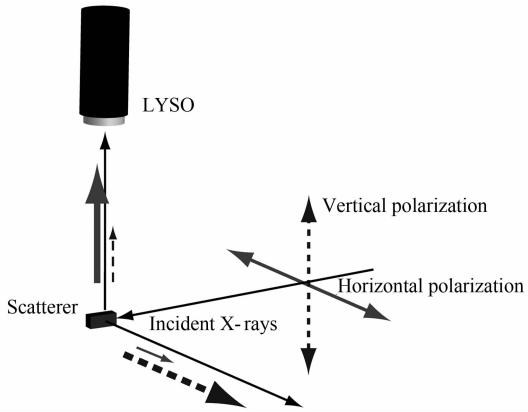

Fig. 10 Schematic diagram of the polarization measurement via the Compton scattering. The LYSO scintillator is mounted perpendicular to the horizontal plane.

In order to see the polarization property of the generated X-rays, we make the intensity measurements of the Compton scattering of the generated X-rays with the horizontal and vertical polarization. The experimental setup is shown in Fig. 10, and the results for each polarization are shown in Fig. 11. The intensity of the Compton scattering with horizontally polarized X-rays is larger than that with vertically polarized X-rays. Therefore, it is concluded that the generated X-rays are polarized with the definite polarization direction according to the laser polarization direction.

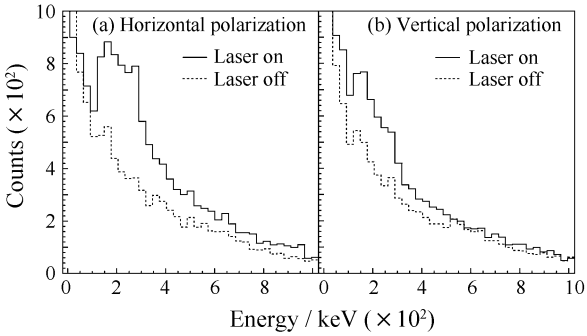

Fig. 11 Result of the Compton scattering measurement. (a) incident X-rays are horizontally polarized. (b) incident X-rays are vertically polarized.

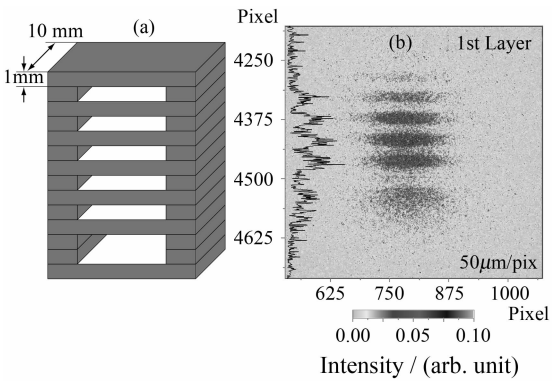

Fig. 12 (a) Imaging object made of lead, (b) the result of the X-ray imaging. As a shield, the lead sheet with the thickness of 1 mm is installed before the imaging plate.

As one of simple applications of the generated X-rays, we make an imaging experiment for an object made of heavy elements by shielding with a lead sheet. The imaging object and result are shown in Fig. 12. We show the possibility the generated X-rays to use for non-destructive imaging of a shielded object.

4 Summary

We show the new Compton backscattered photon sources in MeV and sub-MeV energy range. These photon sources have not been reached a level for practical use yet, but we believe that they will be useful for nuclear physics, materials science, and other scientific purposes after more developments such as increasing the laser-electron interaction length and optimizing the transport of the laser and the electron beam. The details of these developments are published in the Refs. [6, 7].

References:

[1] Nakano T, Ahn J K, Fujiwara M, *et al*. Nucl Phys, 2001, A684: 71c.

[2] Litvinenko V N, Burnham B, Emamian M, *et al*. Phys Rev Lett, 1997, 78: 4 569.

[3] Gibson D J, Anderson S G, Barty C P J, *et al*. Phys Plasmas, 2004, 11: 2 857.

[4] Nelson W R, Hirayama H, Rogers D W O. SLAC-265, 1985, UC-32.

[5] Hirayama H, Namito Y. KEK Internal, 1999, 99-5.

[6] Kawase K, Arimoto Y, Fujiwara M, *et al*. Nucl Instr and Meth, 2008, A592: 154.

[7] Kawase K, Kando M, Hayakawa T, *et al*. Rev Sci Instr, 2008, 79: 053 302.